Chapter 5

Selectivity in Cyclic Polybutadiene Synthesis

5.0 – Abstract

The cis-selectivity in REMP reactions using a family of supported molecular REMP catalysts is explored. A model for cis-selectivity is proposed and evaluated. The synthesis of cyclic and linear PBd analogs through the intentional addition of linear olefin chain transfer agent (CTA) is explored, and their topologies are evaluated using IC. The tether lengths attaching supported molecular REMP catalysts to the surface of SiO_2 were thought to provide selectivity in REMP reactions, but initial evidence was inconclusive. A relationship between *cis* content and catalyst loading is established.

Chapter 5 Acknowledgments

Bob Grubbs, Quan Gan, Alice Chang, Willie Wolf, Dave VanderVelde, Scott Virgil
Anthony Ndiripo and Harald Pasch (U. of Stellenbosch, S. Africa)

5.1 – Introduction

Cyclic Polybutadiene

The ratio of *cis* and *trans* olefins in the PBd backbone greatly affects its physical properties, notably transition temperatures and modulus.[1] Industrially, the *cis/trans* ratio is well-controlled through reaction conditions, but mostly through catalyst design. Traditional alpha-olefin polymerization catalysts produce high-*trans* PBd and anionic polymerization strategies produce high-*cis* PBd (Fig 5.1)

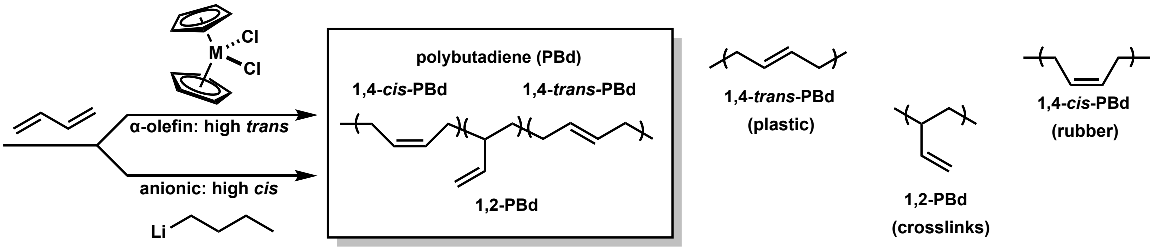

Figure 5.1 | Modulating PBd physical properties through control of *cis/trans*.

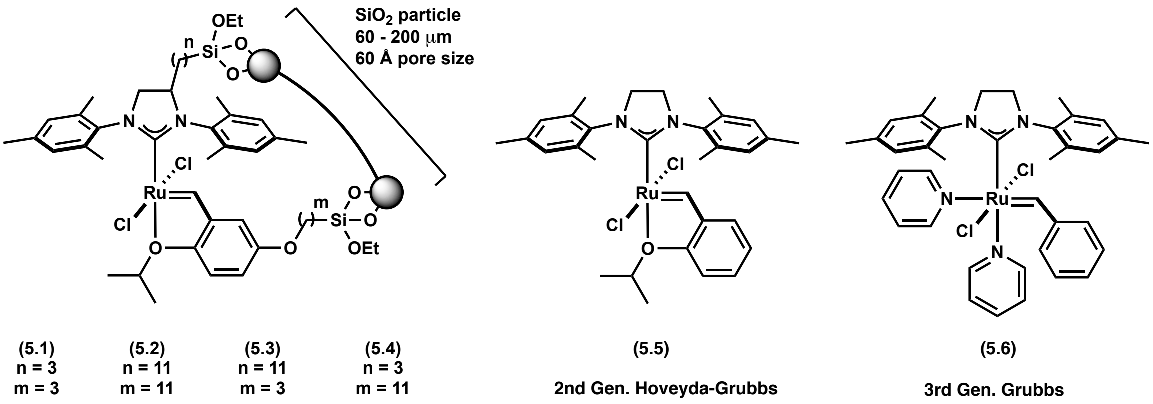

Figure 5.2 | Metathesis catalysts used in the work described herein.

The previous chapter discussed the successful synthesis of multi-gram quantities of cyclic PBd—using supported molecular REMP catalysts **5.1 – 5.4** (Fig 5.2)—and its unexpected high *cis* content, relative to ROMP-derived linear PBd from catalysts **5.5 – 5.6** (Fig 5.3). This chapter will explore the origins of this selectivity, and also various methods to control the MW and D of cyclic PBd.

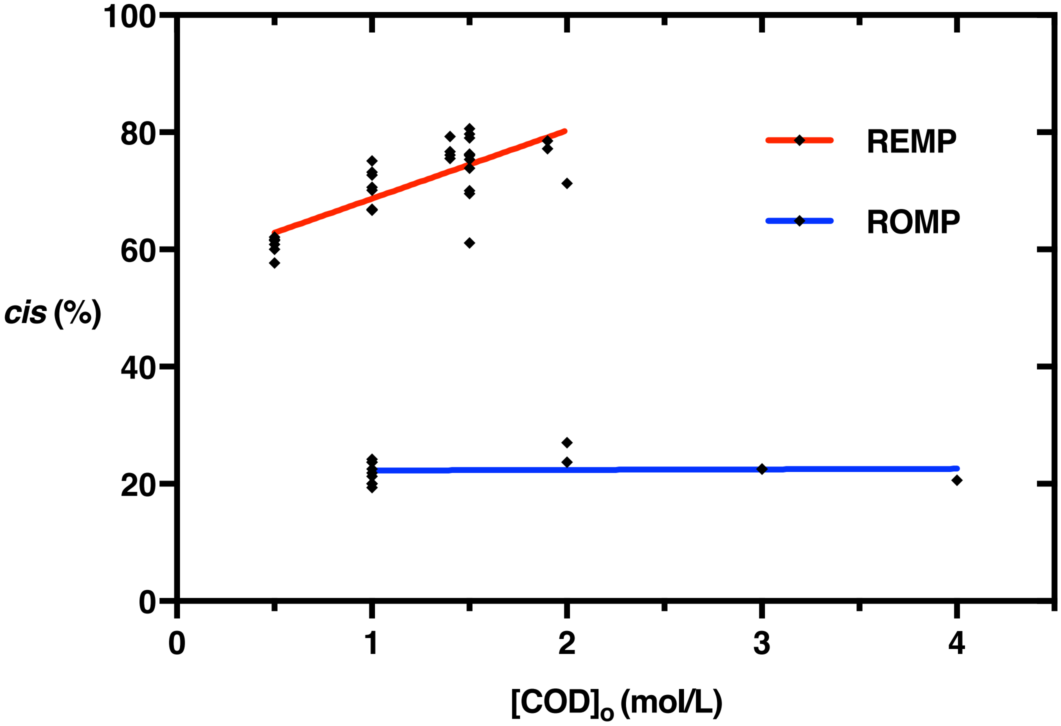

Figure 5.3 | The concentration dependence of *cis* content for REMP of COD compared to the concentration independence of *trans* content for ROMP of COD.

In addition to the *cis* content, the COD REMP reactions discussed in the previous chapter invariably produced PBd with Mn = 190 – 260 kDa. Controlling the microstructure and MW of polymers is a fundamental and recurring challenge in polymer synthesis, so efforts were also undertaken to control M_n of PBd, which will also be discussed in this chapter.

5.2 – Results and Discussion

Initial Investigations of Selectivity in REMP

We developed a model for *cis* selectivity around the relative frequency of secondary metathesis events during REMP: intramolecular chain transfer and intermolecular chain transfer. The former releases a PBd chain from the catalyst and the latter combines to PBd chains into a higher MW species which is still attached to the supported molecular REMP catalyst (Fig 5.3). As shown, this model describes a fundamental *cis*-selectivity of the supported catalyst. We suspected that the SiO_2 surface induced ligand conformations such that a *cis* orientation in the ruthenacyclobutane intermediate was preferred—this is the same general principle which governs the *cis*-selective homogeneous metathesis catalysts developed by our group, and others. Again, this rests upon the assumption that intramolecular chain transfer of cyclic PBd into an actively growing chain occurs much less frequently than the intermolecular chain transfer which releases a cyclic PBd chain into the bulk mixture. In order for the *cis* content to become comparable to the 20% *cis* seen in ROMP*,* the red olefins (Fig 5.4) would have to coordinate to the catalyst in order to be isomerized to *trans*. The above ideas framed our strategy for finding answers to the general questions of selectivity during REMP with catalysts **5.1 – 5.4**.

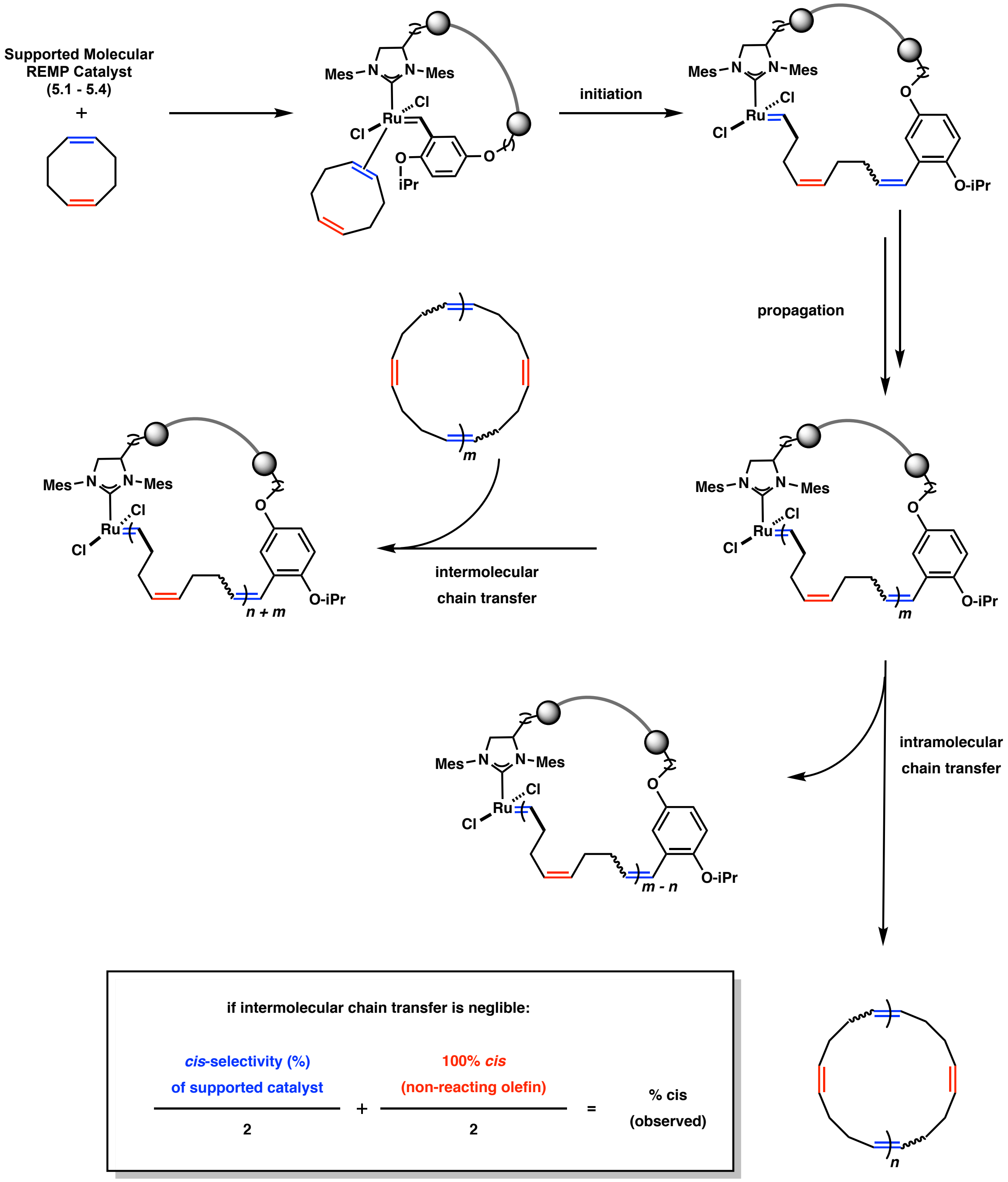

if intermolecular chain transfer is neglible:

$$\frac{\text{cis-selectivity (\%) of supported catalyst}}{2} + \frac{\text{100\% cis (non-reacting olefin)}}{2} = \text{\% cis (observed)}$$

Figure 5.4 | Original model for *cis*-selectivity in REMP of COD.

Along with its *cis* selectivity, the REMP of COD produced PBd with M_n = 190 – 260 kDa. Generally speaking, ROMP catalysts and methods provide excellent control of M_n, so we sought to investigate the preference for this M_n range when catalysts **5.1 – 5.4** were used to REMP COD. In addition to pure curiosity, the overall goal of the project necessitated control *cis/trans* and M_n: to verify the purity of our cyclic polymers via physical property determination, in part using analogous linear polymers as controls.

One general strategy to control microstructure and M_n of PBd was the use of other monomers, namely *cis,trans,trans-* and *trans,trans,trans-*cyclododecatriene (EEZ-CDT and EEE-CDT, respectively). The ring strain and steric profile of CDT isomers varies sufficiently to provide PBd's with significantly different microstructures and M_n's. The three monomers COD, EEZ-CDT, and EEE-CDT all provide PBd via metathesis polymerization, and there exist 3 strategies for controlling PBd properties and topology using these monomers (Fig 5.5). We focused on EEZ-CDT for most experiments because EEE-CDT was not reactive in REMP reactions (Figure 5.6), presumably from a combination of its lower ring-strain and the steric environment surround a reacting *trans* olefin versus a reacting *cis* olefin. Both EEZ-CDT and EEE-CDT were reactive with homogeneous ROMP catalysts **5.5 – 5.6**, however.

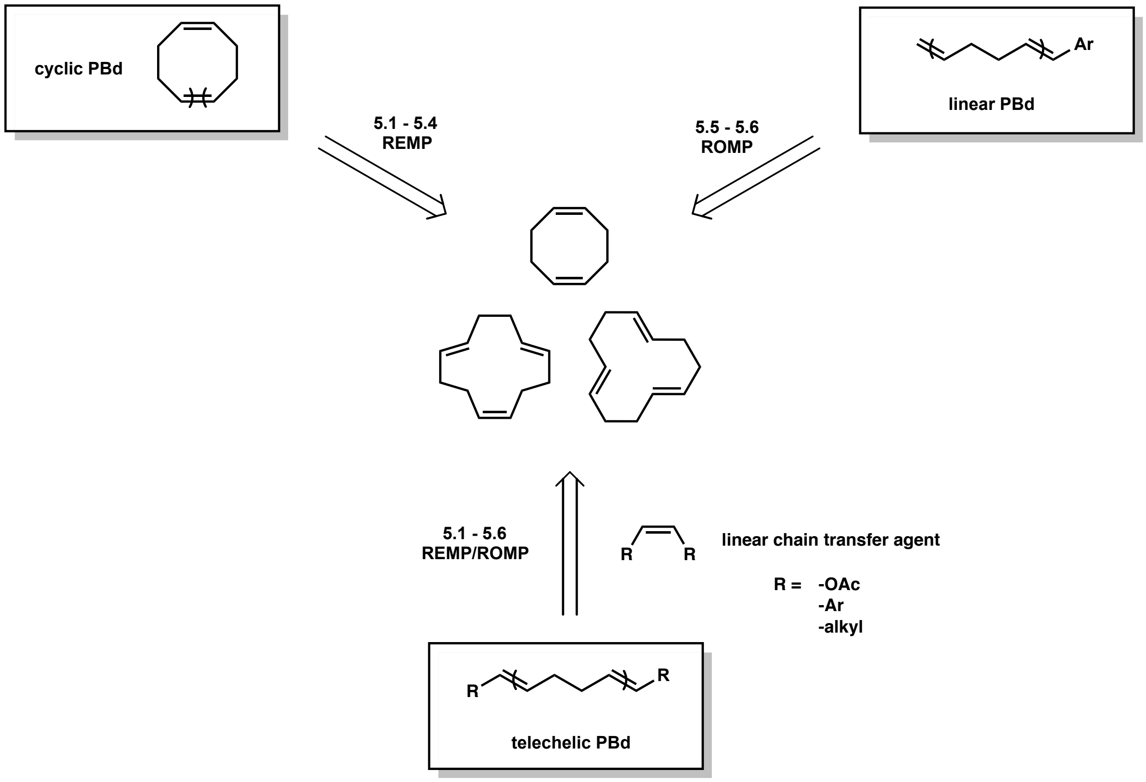

Figure 5.5 | Strategies for preparing cyclic PBd (upper left), linear PBd (upper right), and telechelic PBd, which is also of course linear (bottom).

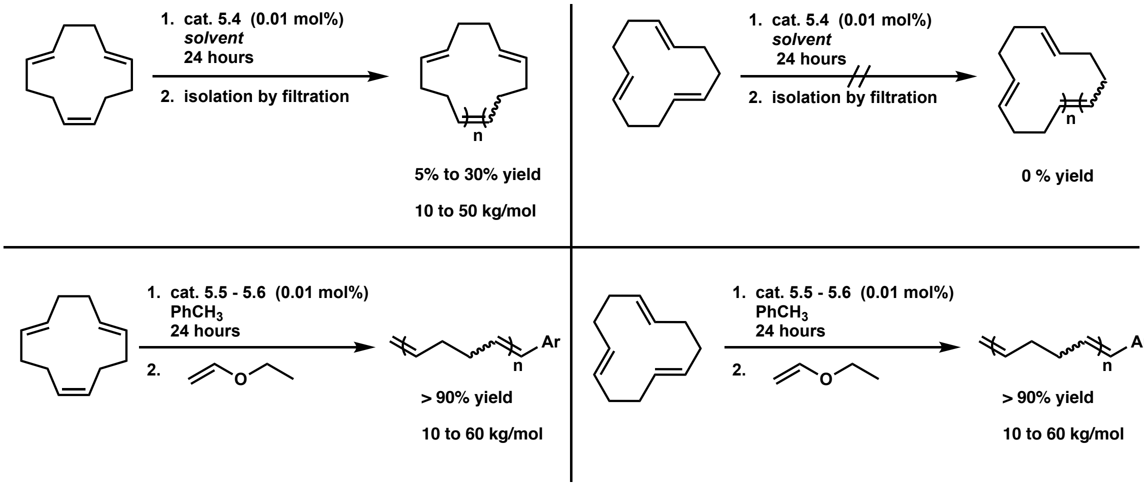

Figure 5.6 | REMP (top) and ROMP (bottom) of both CDT isomers.

The finding discussed in Chapter 3 where 1% ^{t}BuOH/PhCH$_3$ co-solvent system improved the REMP of CP was evaluated again. We also needed to produce multi-gram quantities of cyclic PBd for analysis by rheology and IC, and they had to be lower M_n than the samples described in Chapter 4 in order to simplify analysis and data interpretation. We produced four batches of PBd with REMP catalyst **5.4** using different conditions and delivered them to collaborators for further analysis (Table 5.1). Polymer **5.02** was produced with recycled cat. **5.4** from polymer **5.01**, and Polymer **5.04** was produced with recycled cat. **5.4** from polymer **5.03.** As with the PCP produced in Chapter 3, the ^{t}BuOH led to higher yields, higher M_n, and lower $Đ$. The GPC elution profiles were markedly different for **5.01 – 5.02** versus **5.03 – 5.04** (Figure 5.7).

Table 5.1 | REMP of EEZ-CDT to cyclic PBd using catalyst **5.4** under varying solvent conditions. [a]Determined by ^{13}C NMR.

entry	solvent	cis[a] (%)	M_n (kg/mol)	$Đ$ (M_w/M_n)	yield (%)
5.01	PhCH$_3$	30	1.8	1.9	17
5.02	1% H$_2$O / PhCH$_3$	34	1.7	1.8	13
5.03	1% ^{t}BuOH / PhCH$_3$	13	5.1	2.0	71
5.04	1% ^{t}BuOH / PhCH$_3$	13	3.8	2.1	37

These samples were the first of our PBd samples analyzed through IC, and the elution conditions necessary to separate these samples required considerable effort to develop. The first solvent gradient attempted, Gradient 1 (Fig 5.7), was sufficient to indicate considerable topological heterogeneity in **5.03 – 5.04**, although **5.01 – 5.02** appeared completely topologically homogeneous (Fig 5.8). In order to enhance the topological separation, more sophisticated gradients were explored (Fig 5.9) using **5.04** as the analyte. Polymer 5.04 was chosen because it appeared to be the least topologically pure, so would be a good benchmark for the efficiency of the desired separation conditions. The data presented in Figures 5.9 – 5.16 illuminate two critical successes of this work: we achieved highly pure cyclic PBd and demonstrated the power of IC in topological characterization of macromolecules. Figures 5.11 and 5.12 show the importance of choosing an appropriate solvent system for efficient separation, which is unfortunately not universal for all topologically distinct macromolecules.

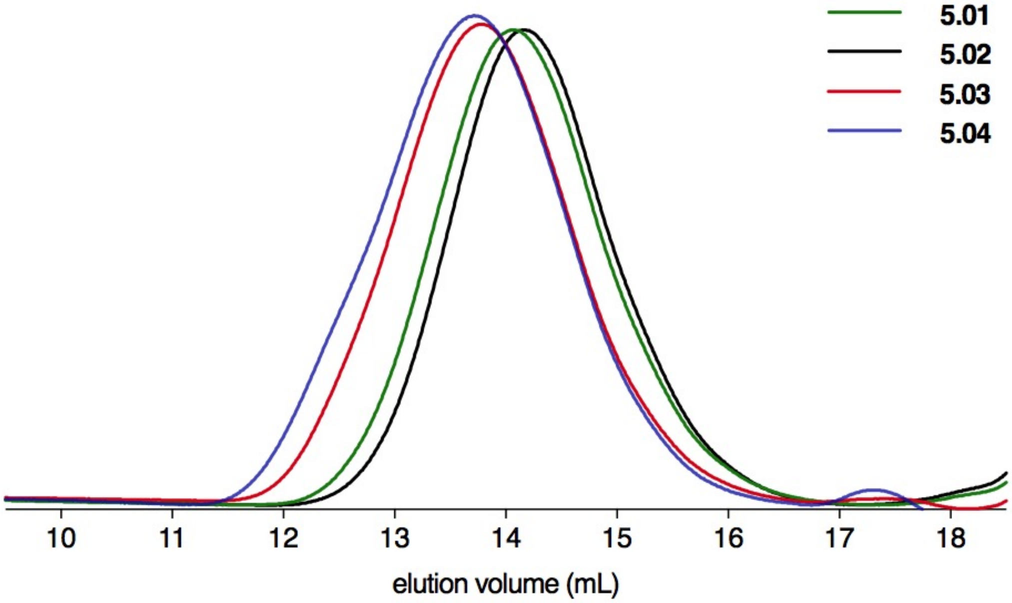

Figure 5.7 | GPC elution profiles for PBd's **5.01 - 5.04**.

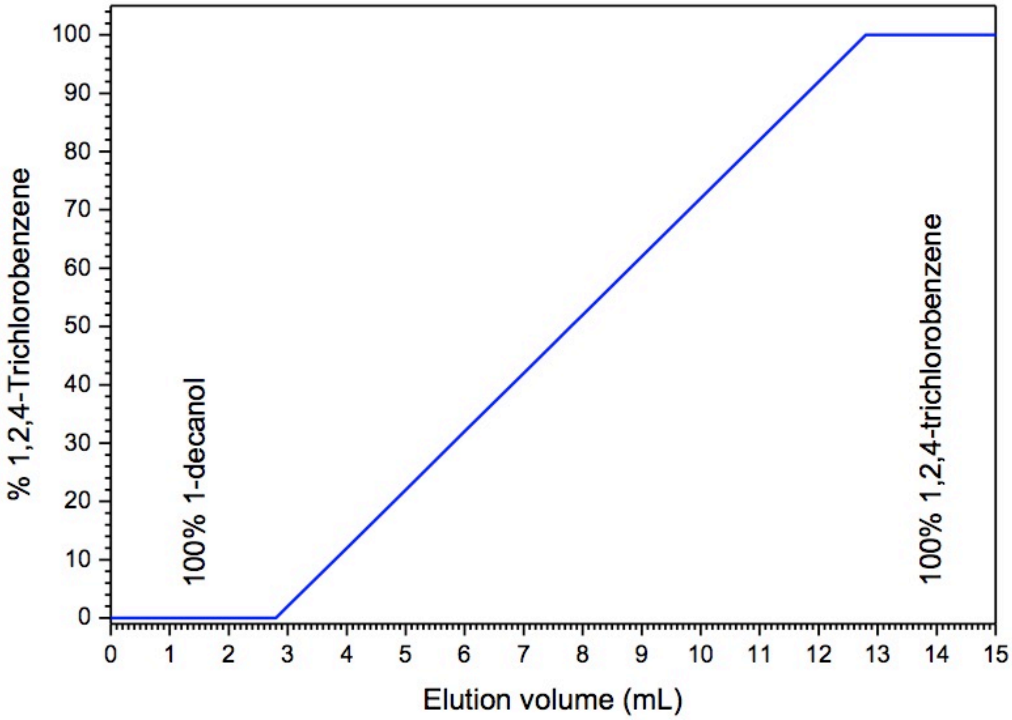

Figure 5.8 | Gradient 1 (blue line) used in IC separation of PBd's **5.01 – 5.04**.

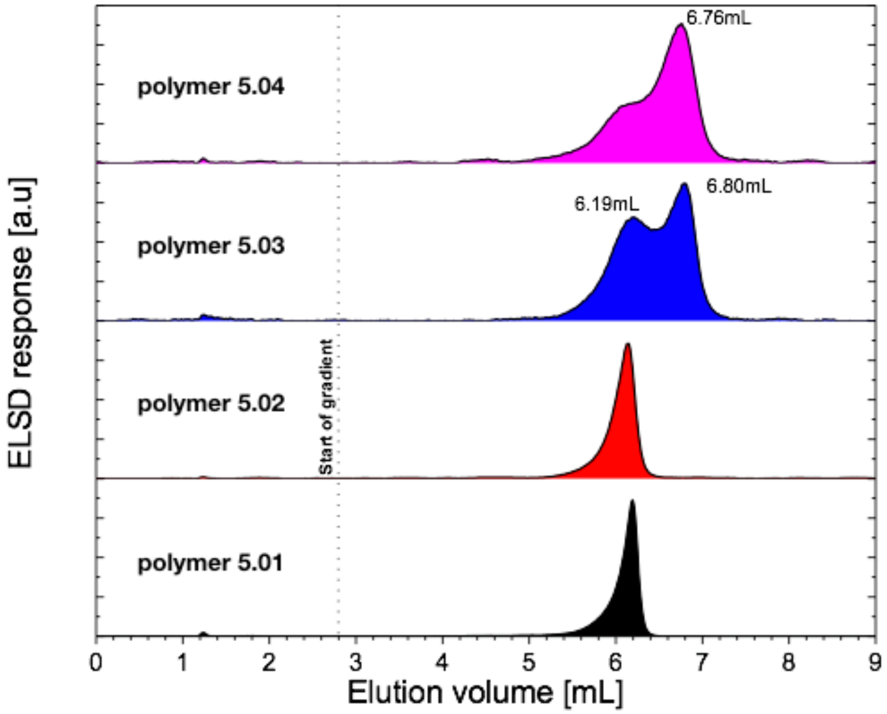

Figure 5.9 | The IC elution profiles for **5.01 – 5.04**. Quantified by normalized evaporative light-scattering detector instrument response.

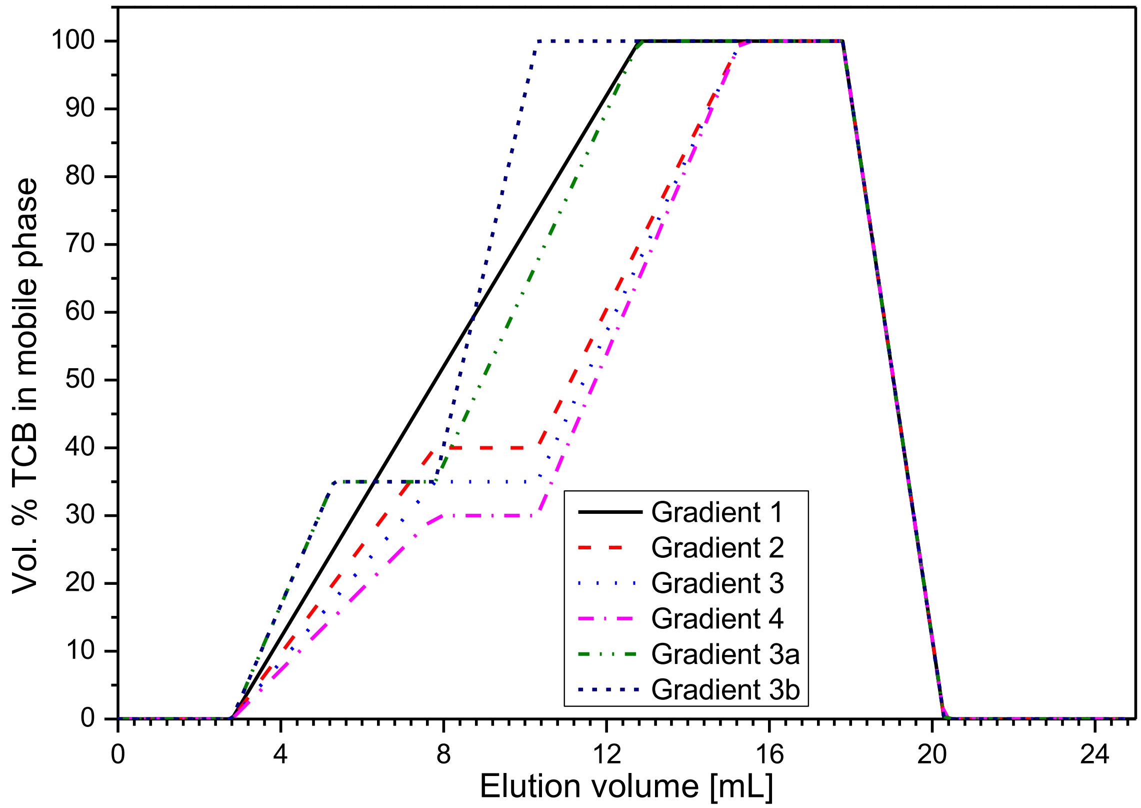

Figure 5.10 | IC elution gradients explored for PBd separations. Eluent consisted of 1-decanol / 1,2,4-trichlorobenzene.

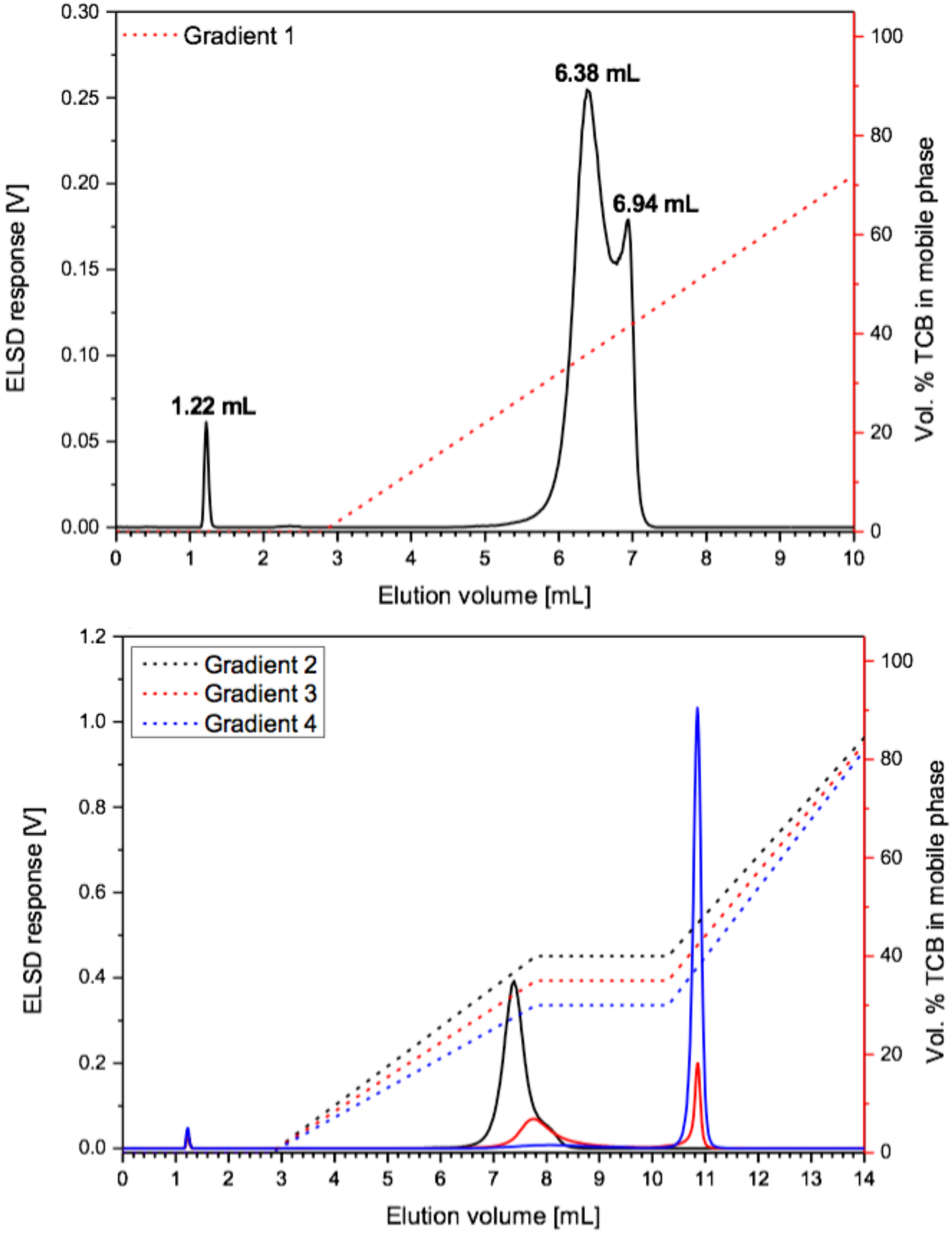

Figure 5.11 | Elution gradient 1 (top) and comparison of elution gradients 1 – 3 (bottom), all with polymer **5.04.**

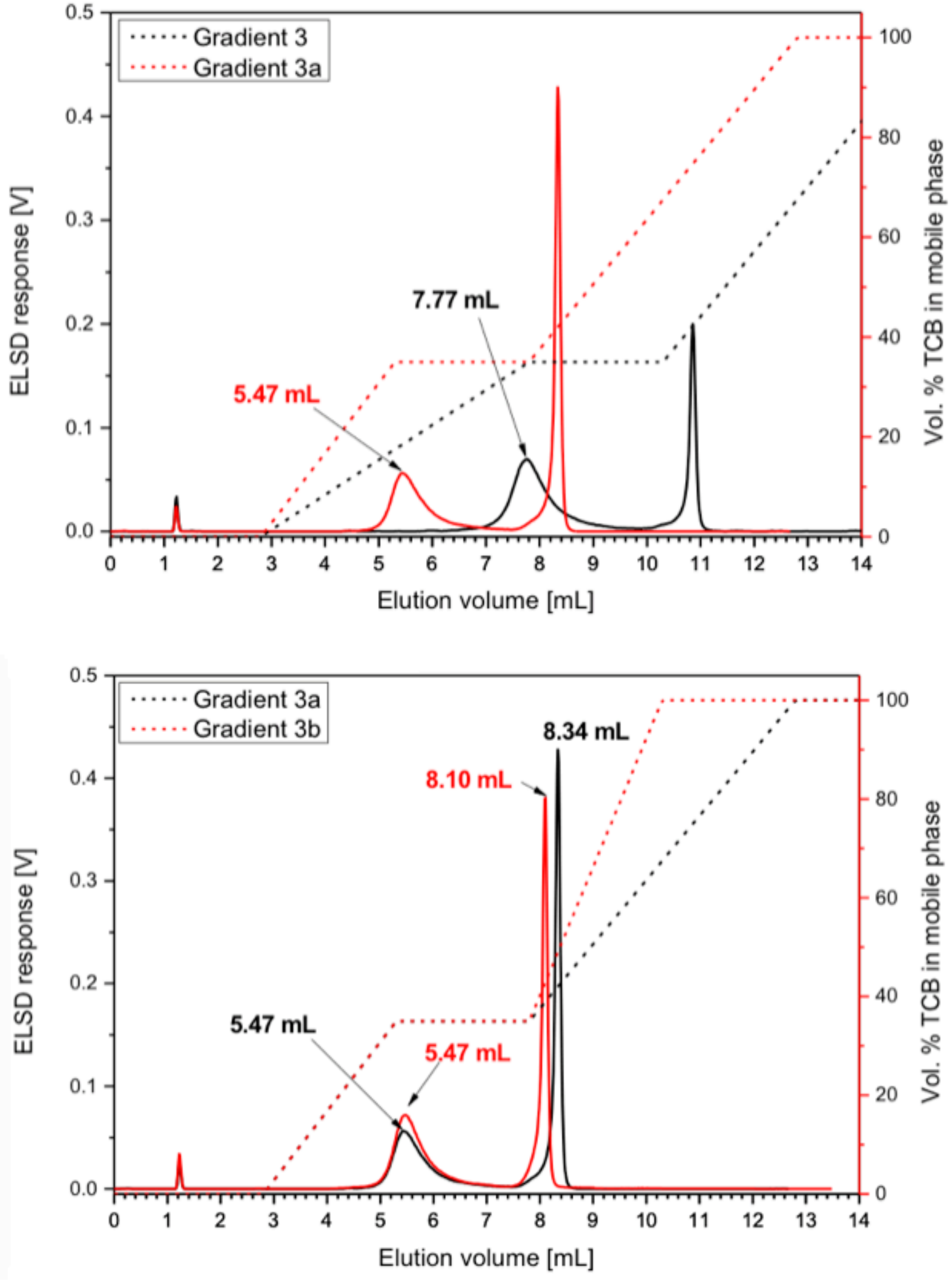

Figure 5.12 | Elution gradients 3 and 3a (top) and elution gradients 3a and 3b (bottom), all with polymer **5.04.**

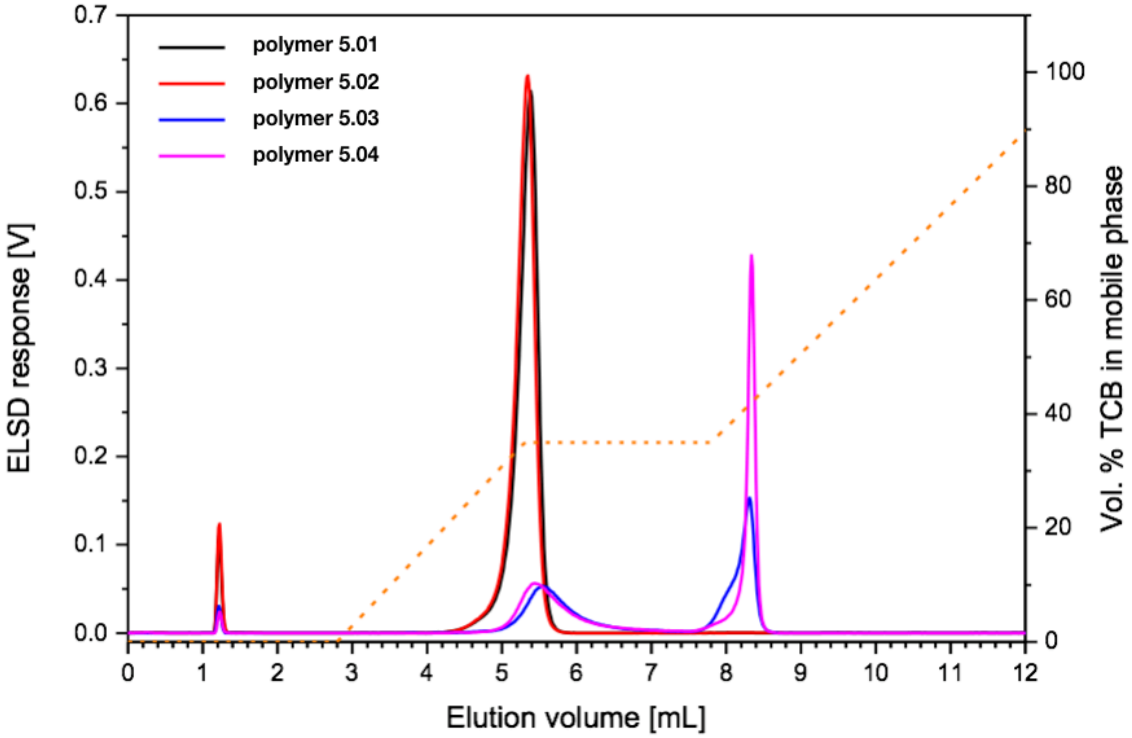

Figure 5.13 | Gradient 3a IC separation of PBd's 5.01 – 5.04. Unretained material at 1.2 mL was small molecule impurity (present in all samples).

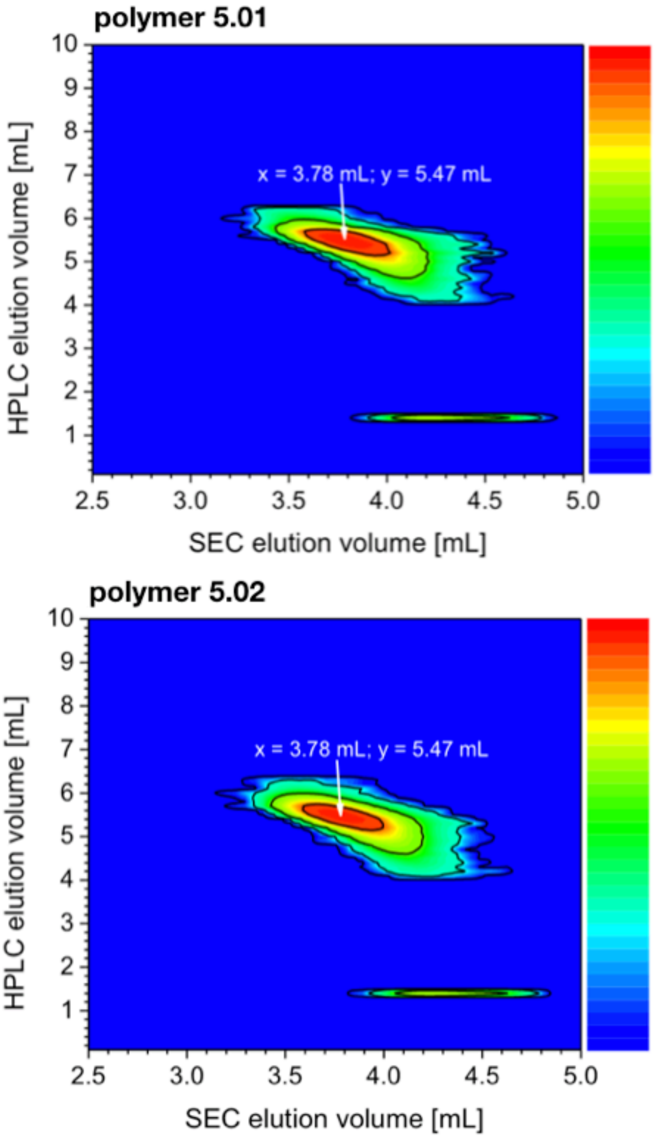

Figure 5.14 | 2D IC-SEC plots for polymers **5.01 – 5.02** with logarithmic color bar scale.

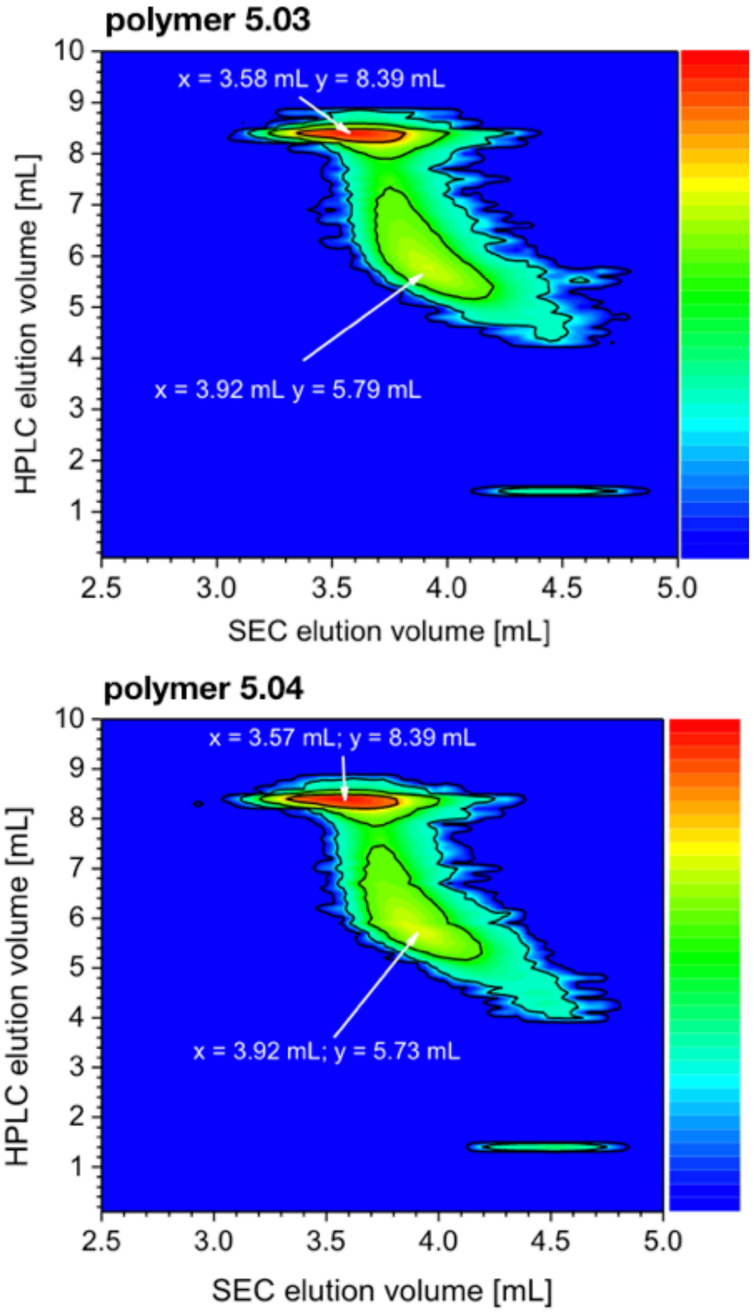

Figure 5.15 | 2D IC-SEC plots for polymers **5.03 – 5.04** with logarithmic color bar scale.

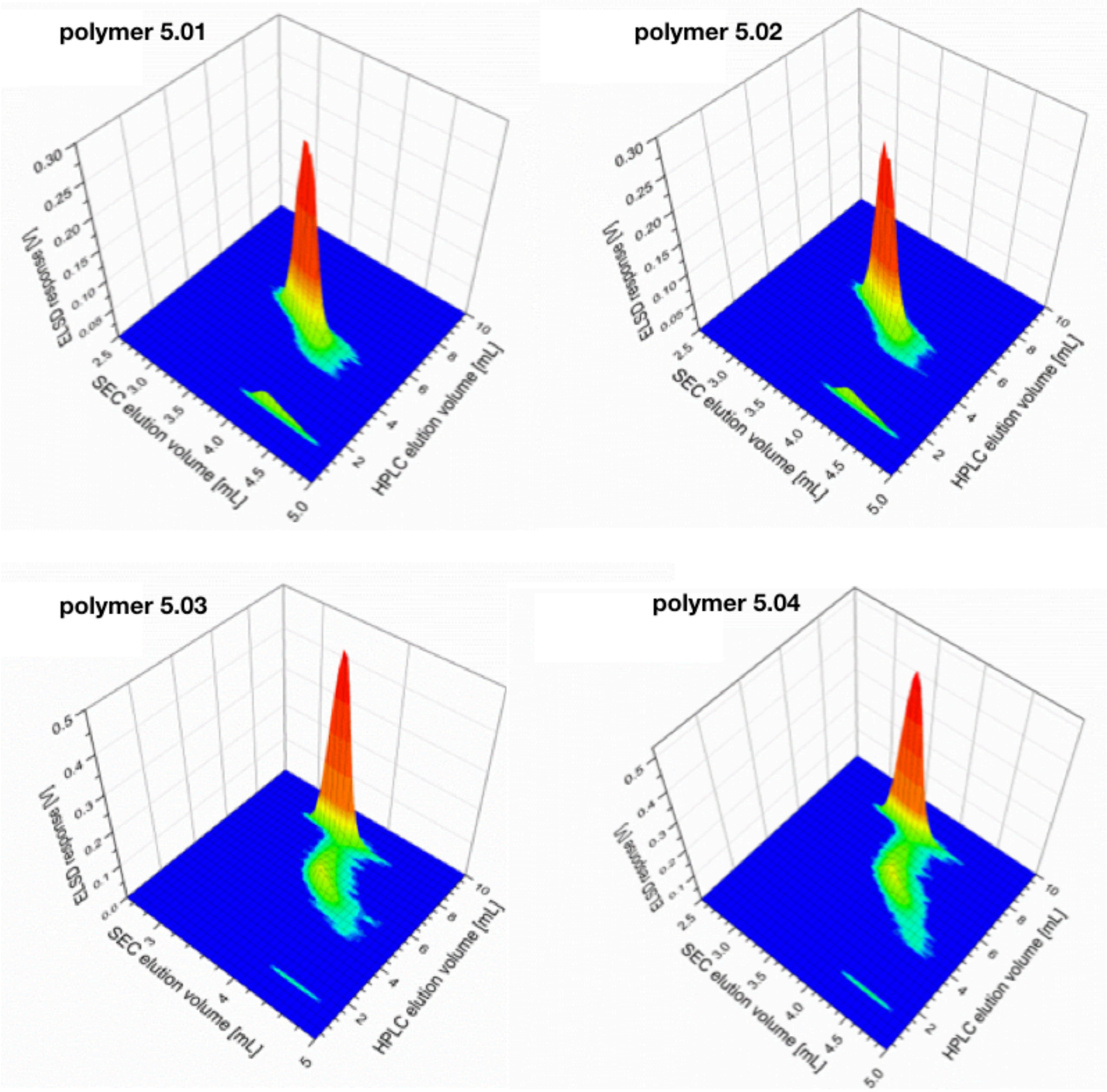

Figure 5.16 | 3-D plot of the IC data shown in Fig 5.14 and 5.15.

Despite the topological impurity of PBd synthesize with the tBuOH/PhCH3 co-solvent system, the polymerization was otherwise better: higher MWs achieved and lower D. Visually, the ^{t}BuOH caused the SiO_2 catalyst particles to disperse more evenly in the polymerization medium. We believe this likely occurs due to H-bonding of tBuOH with the -OH terminated SiO_2 surface which forms solvent shells and prevents particle aggregation. We attempted to optimize REMP of EEZ-CDT using various solvents and conditions, including the use of the more electronegative aromatic solvents chlorobenzene, dichlorobenzene, m-xylene and fluorobenzene; benzene, without a dipole, was also investigated (Table 5.2). Quite unfortunately, we were unable to reproduce the positive results of the tBuOH co-solvent using any other conditions. The GPC elution profiles show that polymers **5.9 – 5.13** were lower MW and higher D than polymer **5.03** (Fig 5.17).

Table 5.2 | Small-scale REMP optimization experiments (all with 0.01 mol % catalyst **5.4**.

entry	$[\mathrm{CDT}]_0$ (mol/L)	solvent	yield (%)	cis[a] (%)	M_n (kg/mol)	$Đ$ (M_w/M_n)	reaction time (hour)
5.1	1.0	$\mathrm{PhCH_3}$	7	30	1.8	2.4	24
5.2	1.5	$\mathrm{PhCH_3}$	13	36	1.7	1.9	24
5.3	2.0	$\mathrm{PhCH_3}$	15	36	5.1	3.9	24
5.4	3.0	$\mathrm{PhCH_3}$	23	34	3.8	6.2	24
5.5	5.4	$\mathrm{PhCH_3}$	20	30	26.3	1.8	66
5.6	5.4	$\mathrm{PhCH_3}$	10	33	14.0	1.8	66
5.7	5.4	$\mathrm{PhCH_3}$	6	35	11.5	2.0	66
5.8	5.4	$\mathrm{PhCH_3}$	11	34	13.5	1.8	66
5.9	3.0	PhH	11	33	16.6	1.7	24
5.10	3.0	$\mathrm{C_6H_5Cl}$	6	36	16.6	1.8	24
5.11	3.0	$\mathrm{C_6H_4Cl_2}$	4	36	11.8	1.7	24
5.12	3.0	*m*-$\mathrm{Ph(CH_3)_2}$	10	34	20.5	1.9	24
5.13	3.0	$\mathrm{C_6H_5F}$	12	35	21.8	1.9	24

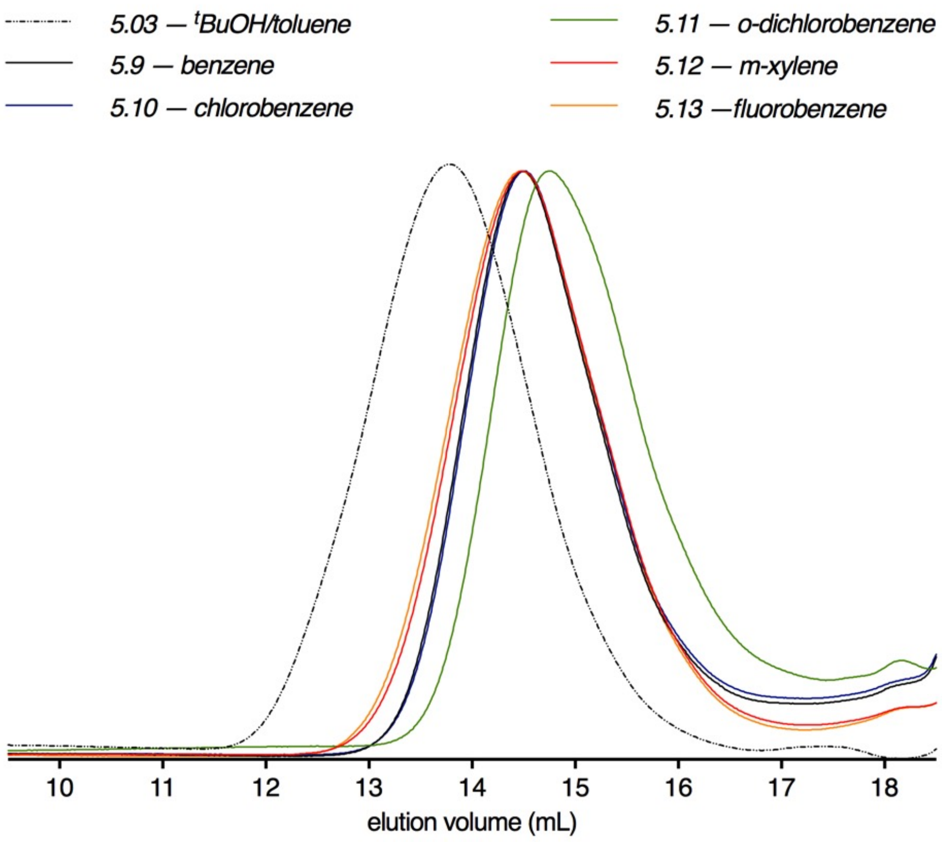

Figure 5.17 | GPC elution profiles (dRI traces) for EEZ-CDT-derived PBd prepared with REMP catalyst **5.04.**

Cyclic and Linear PBd Analogs

We were largely unsuccessful in gaining control of material properties of PBd produce with REMP of EEZ-CDT using catalyst **5.4.** We then shifted our focus to the synthesis of linear PBd analogs using the supported molecular REMP catalysts, instead of homogeneous ROMP catalysts **5.5 – 5.6.** The obvious route to linear polymers is to ROMP COD or CDT using a homogeneous ROMP catalyst, but we decided to take advantage of the chain cleavage caused by incorporation of linear chain transfer agent (CTA) during REMP (Fig 5.18). This process is, of course, detrimental when synthesizing cyclic polymers, but we felt this strategy would be the best control for making perfect cyclic/linear analogs since they could be *cis/trans* and MW matched if polymerized with the same catalyst.

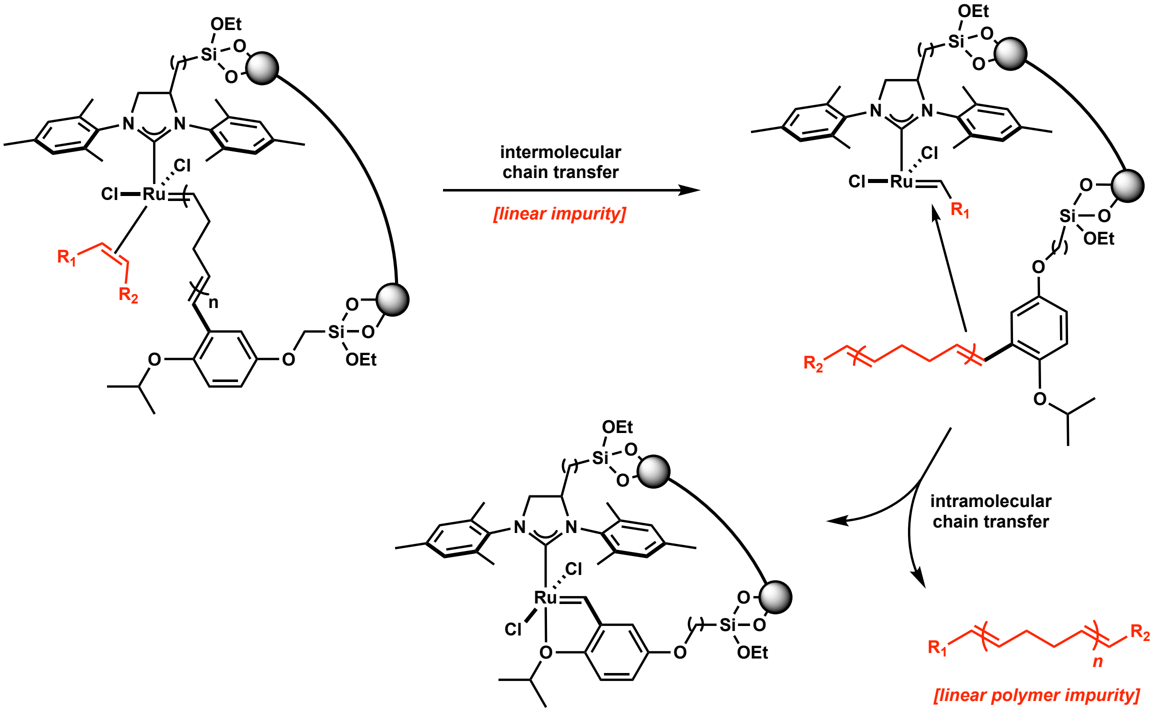

Figure 5.18 | The process during REMP where linear CTA (red) causes chain cleavage and a linear polymer (red, bottom right).

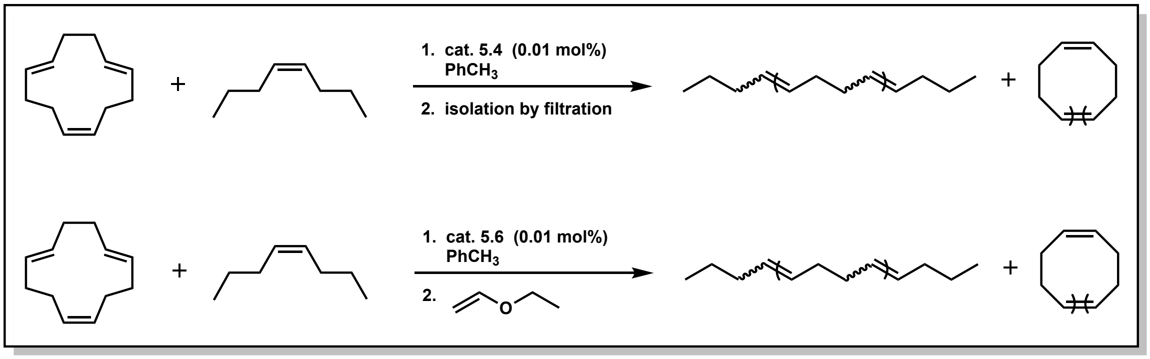

Figure 5.19 | Synthesis of cyclic and linear PBd analogs using *cis*-4-octene.

We synthesized cyclic and linear PBd using **5.4** and **5.6** with varying amounts of the CTA *cis*-4-octene (Figure 5.19). By monitoring Mn vs. [*cis*-4-octene]$_0$, we were able to get a sense for the relative ration cyclic:linear in the PBd produced. Because the Mn of a cyclic chain does not chain when one *cis*-4-octene molecule inserts into the backbone, there was a threshold [*cis*-4-octene]$_0$ where a M_n change would be observed**.** Our initial experiments were according to the scheme in Fig 5.19, bottom, using homogeneous cat**. 5.6** (Fig 5.20). We were able to gain control of Mn through variable reaction time and equivalents of added CTA.

The addition of CTA to REMP reactions then proceeded according to the scheme in Fig 5.20, top. According to our initial assumptions about the system, we hoped to see a gradual decrease in Mn as more equivalents of CTA were added (Fig 5.21, top, polymers **5.14 – 5.19**). This experiment was mostly successful, as the control without CTA eluted first, and the PBd with the most added CTA eluted last. However, the intermediate entries eluted somewhat unpredictably. We elected to repeat this experiment using the exact same conditions (Fig 5.21, bottom, polymers **5.20 – 5.25**). Fortunately we were able to see a predictable trend in GPC elution profiles depending on added CTA. These samples were being analyzed by IC and rheology at the time this dissertation was submitted.

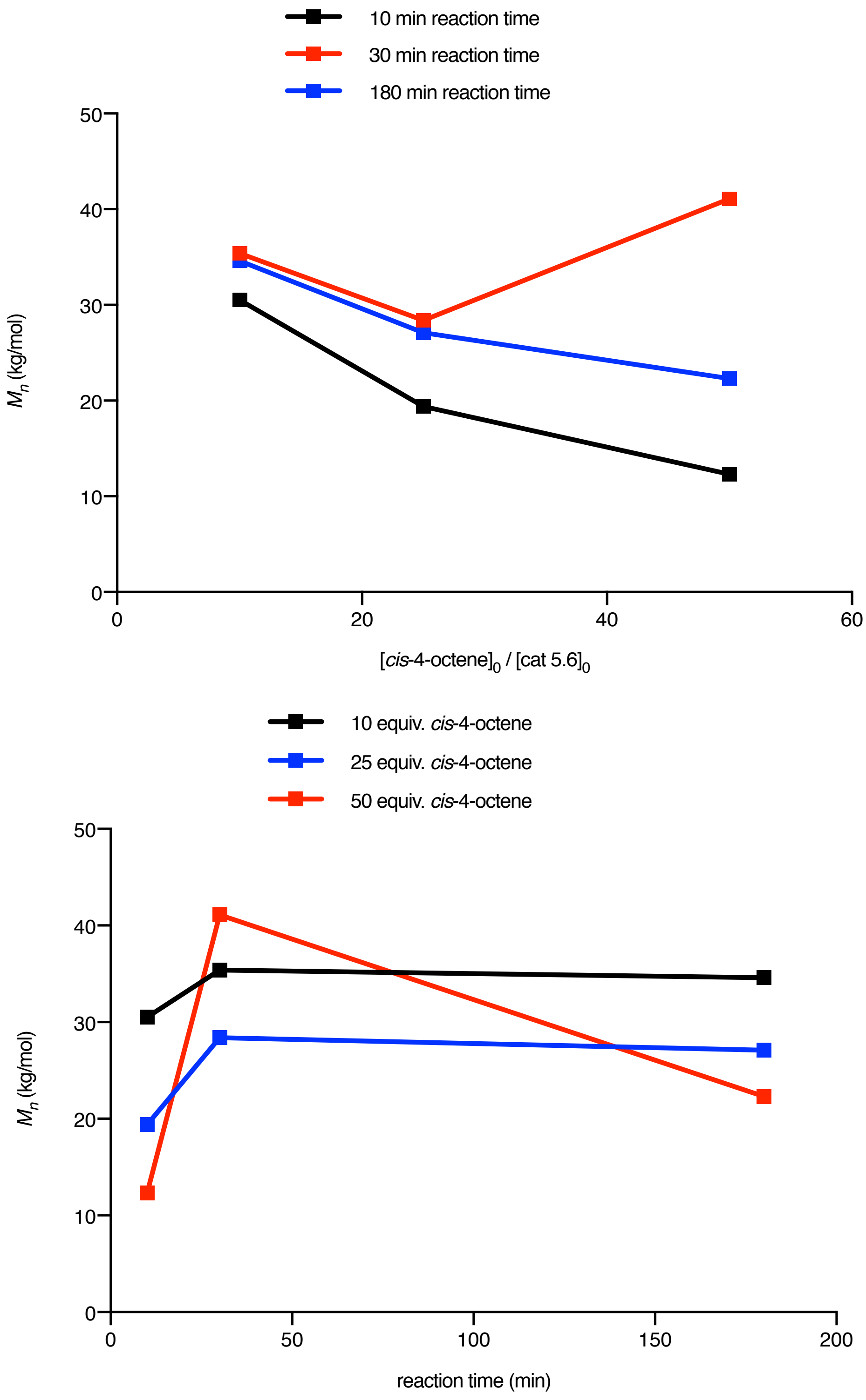

Figure 5.20 | M_n control through [*cis*-4-octene]$_0$ and reaction time.

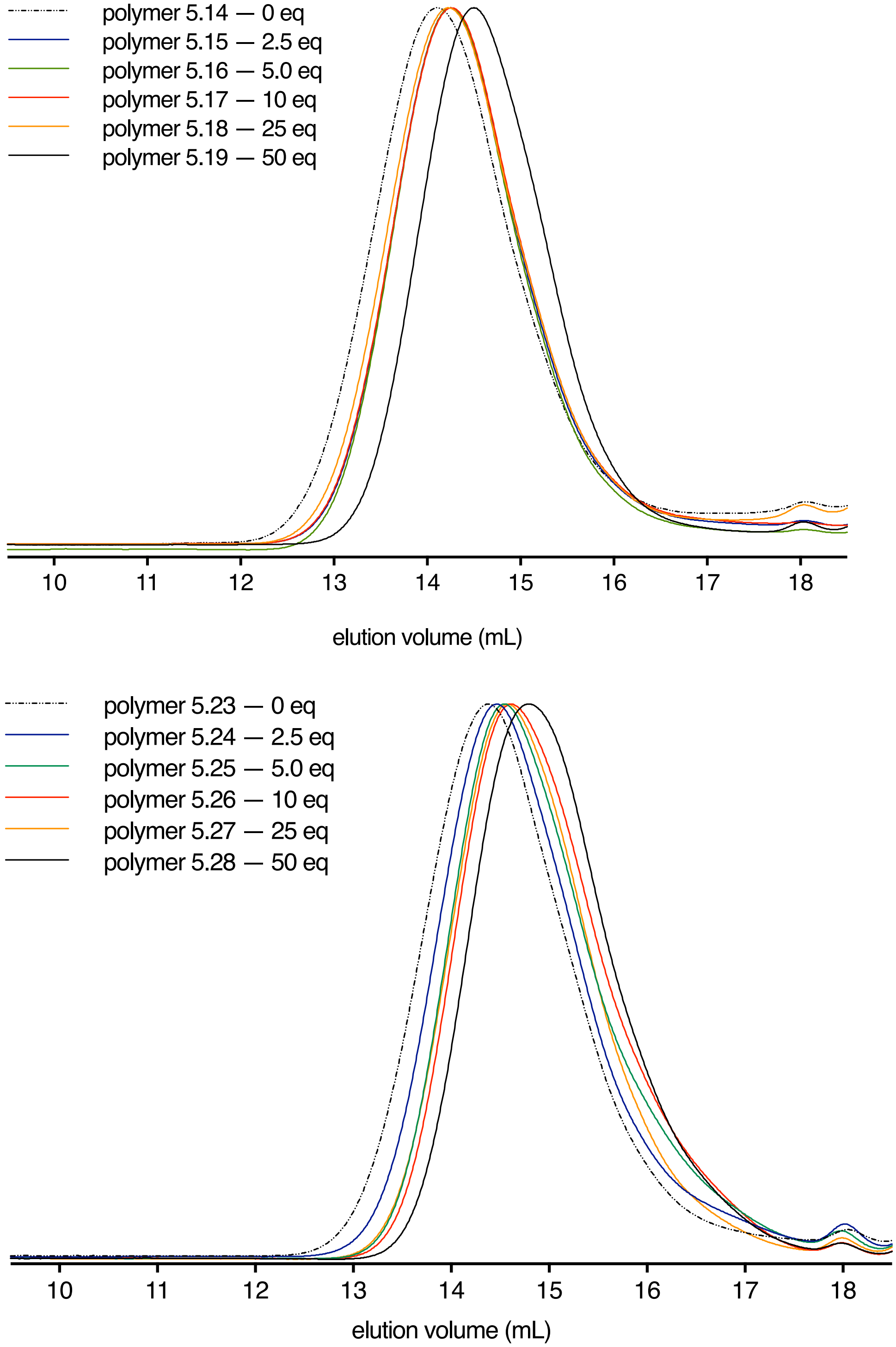

Figure 5.21 | GPC elution profiles of a series of REMP reactions with progressively more eq. of *cis*-4-octene (polymers 5.14 – 5.27 top), and their duplicates (polymers (5.23 – 5.28).

Effect of REMP Catalyst Tether Lengths

As discussed previously, the means to control MW and microstructure in cyclic PBd would be a significant advance in our efforts to improve our REMP methodology. We suspected the tether lengths from NHC ligand and isopropoxy chelate on our supported molecular REMP catalysts **5.1 – 5.4** could provide some degree of control over material properties. The tether length with the original homogeneous REMP catalysts was shown to greatly affect polymerization profiles.[2] The distance of the active Ru catalytic site from the SiO_2 surface might affect the rates of monomer incorporation and inter- and intramolecular chain transfer, and thus affect the MW and *cis* content. We investigated this through a series of REMP reactions using catalysts **5.1 – 5.3** polymerize COD at variable concentrations, reaction times, and catalyst loadings (Table 5.3).

Polymers **5.29 – 5.38** (Table 5.3) were characterized using GPC and ^{13}C NMR to determine the molecular weight distributions and *cis/trans* isomerism, respectively. The dependence of *cis* content on $[COD]_0$ was previously observed (Fig 5.3), but we were not able to find this relationship in these experiments. For all concentrations explored (0.5 M, 1.0 M, and 2.0 M), the *cis* content fell between 70% and 78%, unlike the 58% to 82% range we previously observed. Higher concentrations—above 2.0 M—may provide higher *cis* content, but these experiments have not yet been pursued. Polymer **5.32**, however, had a *cis* content far below the others, at 41%. The reaction time (1440 min) and low concentration

(0.5 M) of this reaction led to more instances of chain transfer and *cis*-degradation towards the thermodynamic ratio of 20% *cis,* which is frequently observed for homogeneous metathesis reactions.[3-5] Our previous model of *cis*-selectivity in REMP (Fig 5.4) suggested chain transfer events may have little to no effect on *cis/trans*, but we believe this may not be the case, particularly at lower concentrations. The inherent *cis* selectivity of REMP using catalysts **5.1 – 5.4** may not originate from a steric effect surrounding the ruthenacyclobutane intermediate, but rather, the SiO_2 surface may decrease the frequency of chain transfer events relative to homogeneous catalysts; this phenomenon would be more exaggerated at higher concentrations where diffusion is slower. This is further supported by the elution profiles of polymers **5.29** and **5.32** (Fig 5.24). They were conducted with identical reaction conditions, but **5.32** reacted for 36 times longer. The lower MW region (longer elution time) disappears for **5.32**, likely due to the reincorporation of low MW chains into the active catalyst site, thereby increasing the MW and lowering the D.

Table 5.3 | 15 COD-derived PBd samples prepared under various conditions with catalysts **5.1 – 5.3**. Mw determined by SEC-MALLS and *cis (%)* determined by ^{13}C NMR.

entry	catalyst	catalyst loading (mol %)	$[COD]_0$ (mol/L)	reaction time (min)	*cis* (%)	M_w (kg/mol)	$Đ$ (M_w/M_n)
5.29	5.1	0.01	0.5	40	73	63	3.30
5.30	5.1	0.01	1	40	70	281	1.58
5.31	5.1	0.01	2	40	72	338	1.65
5.32	5.1	0.01	0.5	1440	41	102	1.70
5.33	5.2	0.01	0.5	40	75	35	2.74
5.34	5.2	0.01	1	40	71	301	1.60
5.35	5.2	0.01	2	40	78	428	1.43
5.36	5.3	0.01	0.5	40	74	121	2.13
5.37	5.3	0.01	1	40	72	317	1.47
5.38	5.3	0.01	2	40	74	373	1.52
5.39	5.3	0.025	1.5	120	74	368	1.58
5.40	5.3	0.04	1.5	120	70	272	1.59
5.41	5.3	0.02	1.5	40	73	248	1.42
5.42	5.3	0.0001	5.0	1440	82	483	1.58
5.43	5.3	0.0005	5.0	1080	76	273	1.44

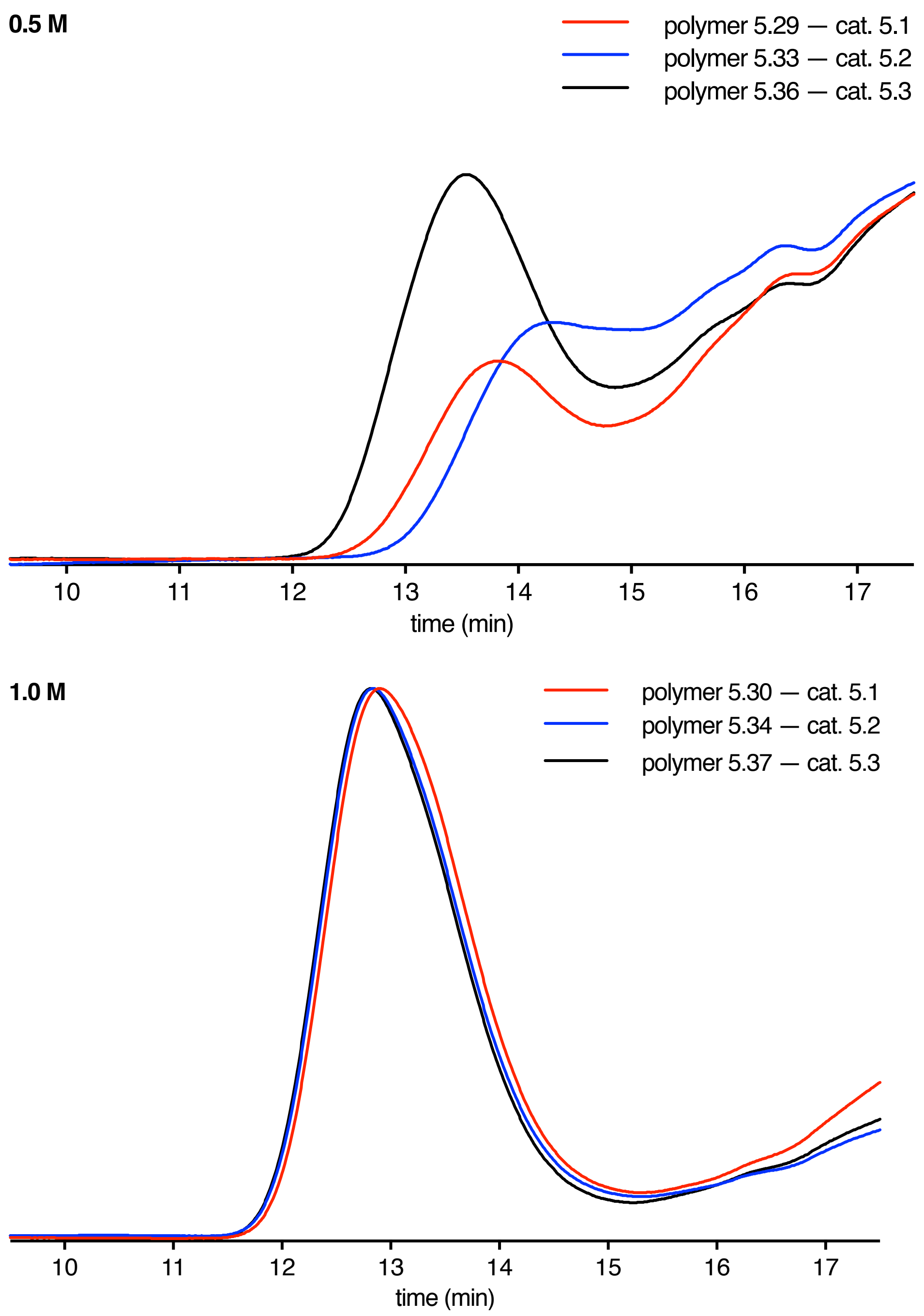

Figure 5.22 | GPC elution profiles of COD REMP using **5.1 – 5.3** at 0.5 M (top), and GPC elution profiles of COD REMP using **5.1 – 5.3** at 1.0 M (bottom).

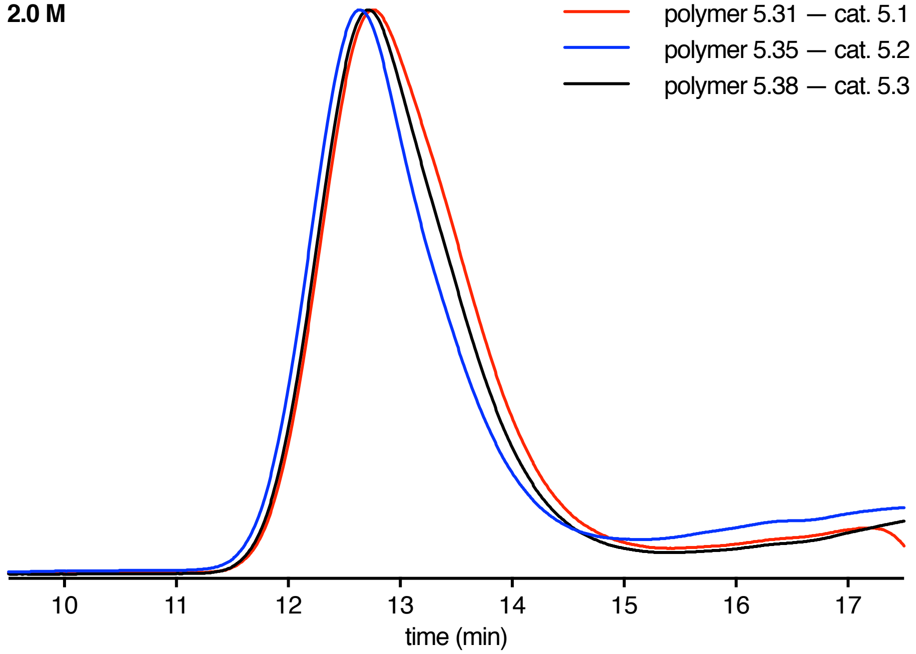

Figure 5.23 | GPC elution profiles of COD REMP using **5.1 – 5.3** at 2.0 M.

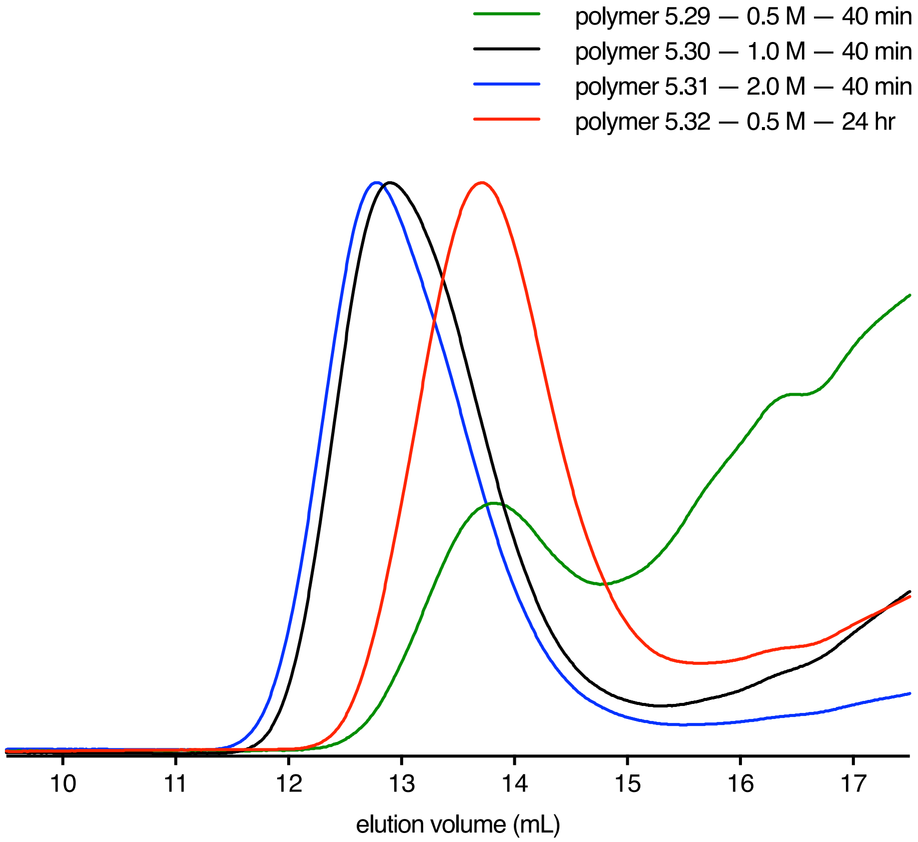

Figure 5.24 | GPC elution profiles of polymers **5.29 – 5.32** prepared with COD and REMP cat. **5.1** at different concentrations and reaction times.

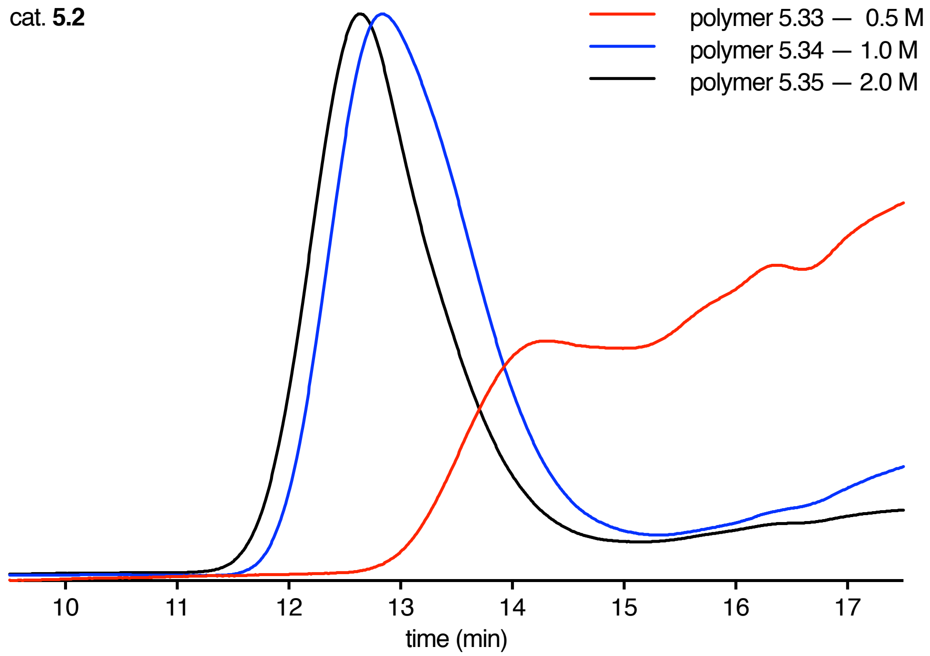

Figure 5.25 | GPC elution profiles of polymers **5.33 – 5.35** prepared with COD and REMP cat. **5.2** at 0.5 M (red), 1.0 M (blue) and 2.0 M (black).

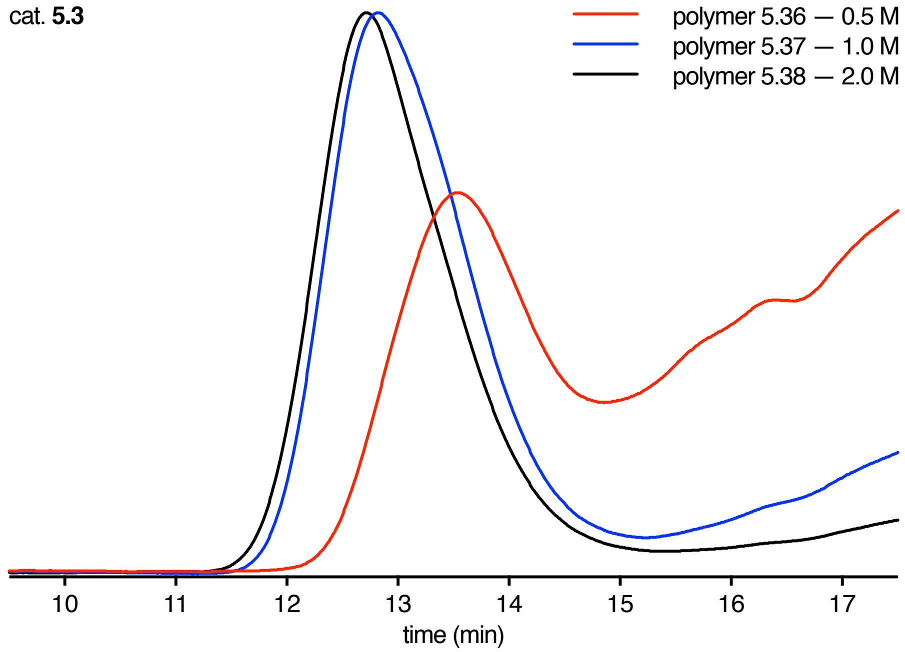

Figure 5.26 | GPC elution profiles of polymers **5.36 – 5.38** prepared with COD and REMP cat. **5.3** at 0.5 M (red), 1.0 M (blue) and 2.0 M (black).

Effects of REMP Catalyst Loading

We further investigated the reactivity and selectivity of REMP catalysts using a broader range of catalyst loading with catalyst **5.3** for COD (Table 5.3, polymers **5.39** – **5.43**). By decreasing catalyst loading, we believed we could decrease the frequency of chain transfer events, and perhaps observe discrepancies in MW and *cis/trans* that we could not observe with higher loadings. Although we did not observe a clear trend with MW vs. catalyst loading as is generally seen with ROMP catalysts,{Grubbs:2004ct} we did see an excellent GPC elution profile for polymer **5.43**, made using 5.0 ppm catalyst **5.3** (Fig 5.27). It also shows a D value of 1.44, which is among the lowest we have seen for cyclic PBd. Additionally, polymer **5.42**, made using 1.0 ppm catalyst **5.3**, reached a M_w of 483 kDa, which is the highest we have achieved for REMP-derived PBd.

These experiments also provided insight into the nature of *cis* selectivity in REMP. Since we suspect the frequency of secondary metathesis chain transfer events dictates the relative rate of *cis*-degradation, we were interested to find a linear relationship between *cis*(%) and log([cat. **5.3**]:[COD]$_0$) (Fig 5.28). This suggests the rate of chain transfer events is directly proportional to the catalyst loading. We may be able to exploit this phenomenon in the future to control *cis/trans* of PBd and other polyolefins, which would be a powerful addition to the growing array of strategies we have to control reactivity and selectivity during REMP reactions.

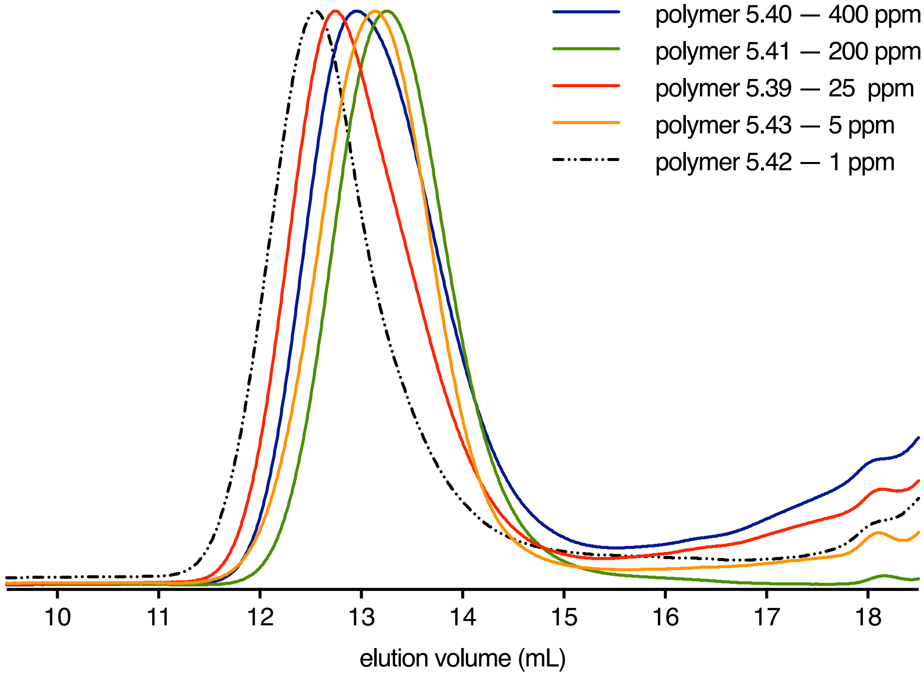

Figure 5.27 | GPC elution profiles of polymers **5.39 – 5.43** prepared with COD and REMP cat. **5.3** using different catalyst loadings ranging from 400 ppm (polymer **5.40**, blue) to 1 ppm (polymer **5.42**, dotted black).

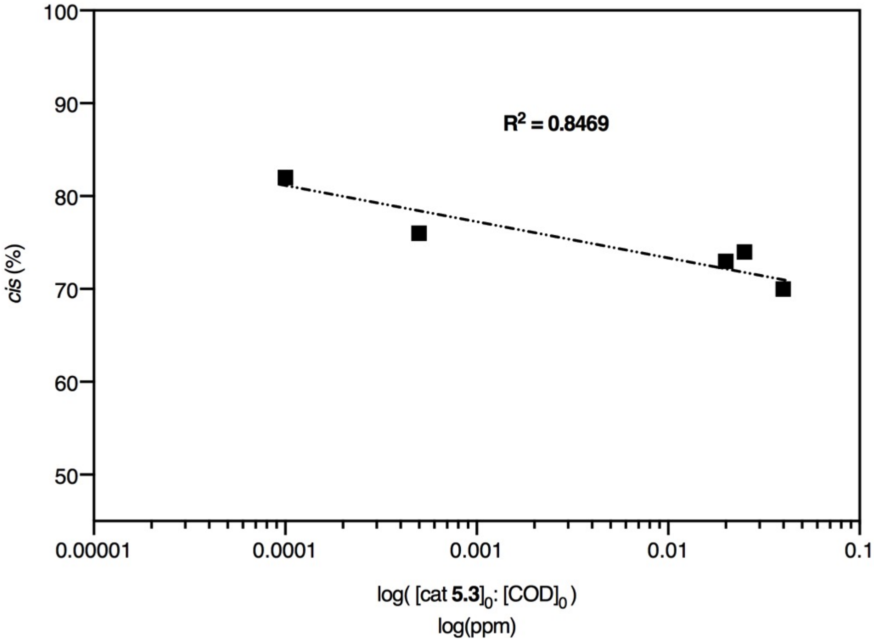

Figure 5.28 | Linear relationship between *cis* and log([cat. **5.3**]:[COD]$_0$)for REMP of COD using catalyst **5.3**.

5.3 – Conclusions and Future Outlook

The investigations into selectivity in REMP reactions discussed in this chapter elucidated the relationship between catalyst loading, *cis/trans* isomerism, MW, Đ, and reaction time. Experimentally determined reaction parameters allowed us to control the material properties of PBd more than was previously possible. CTAs were shown to reduce the MW of PBd during ROMP and REMP reactions with homogeneous and supported catalysts, respectively. Further studies will be required to reveal any selectivities or reactivities unique to any of the 4 supported molecular REMP catalysts based on their tether lengths to the surface of the SiO_2 support.

5.4 – Experimental

General Information

All reactions were carried out in glassware flame-dried in vacuo (100 mTorr) unless otherwise specified. Reactions were performed using air-free Schlenk technique (100 mTorr vacuum and UHP grade 5.0 argon gas) on the benchtop or in a Vacuum Atmospheres glovebox (N_2-filled, O_2 concentration < 0.25 ppm) unless otherwise specified. All solvents were purchased from Sigma-Aldrich (anhydrous, 99.9%) and further purified by passage through solvent purification columns, sparged with argon, and then stored over 4 Å molecular sieves in Strauss flasks, unless otherwise specified.[17] All homogeneous Grubbs catalyst (**3.1 – 3.6**, Fig 3.1) were received as a generous gift by Materia, Inc. (Pasadena, CA) and used without further purification. All other reagents were purchased from Sigma-Aldrich and used as received unless otherwise stated. Room temperature was 18-20 °C for all syntheses described herein.

Size-exclusion chromatography (SEC) data was obtained with an HPLC system consisting of two two Agilent PLgel MIXED-B 300×7.5 mm columns with 10 μm beads, and an Agilent 1260 Series pump and autosampler; the columns were connected in series with a Wyatt 18-angle DAWN HELEOS multi-angle laser light scattering detector and Optilab rEX differential refractive index detector. The mobile phase was either pure THF or stabilized THF (50-150 ppm butylated hydroxytoluene (BHT).

Orbital agitation of REMP reactions was performed using an IKA KS 260 basic flat orbital shaker with a swivel motion (no z-axis motion). Orbital agitation rate varied between 200 and 400 rot/min.

5.4 – References

(1) Brandt, H. D.; Nentwig, W.; Rooney, N.; LaFlair, R. T.; Wolf, U. U.; Duffy, J.; Puskas, J. E.; Kaszas, G.; Drewitt, M.; Glander, S. *Ullmann's Encyclopedia of Industrial Chemistry, 1*, 2nd ed.; Wiley-VCH: Weinheim, Germany, 2000; Vol. 39, pp 30 –32.

(2) Xia, Y.; Boydston, A. J.; Yao, Y.; Kornfield, J. A.; Gorodetskaya, I. A.; Spiess, H. W.; Grubbs, R. H. *J. Am. Chem. Soc.* **2009**, *131* (7), 2670–2677.

(3) Marx, V. M.; Sullivan, A. H.; Melaimi, M.; Virgil, S. C.; Keitz, B. K.; Weinberger, D. S.; Bertrand, G.; Grubbs, R. H. *Angew. Chem. Int. Ed.* **2015**, *54* (6), 1919–1923.

(4) Endo, K.; Grubbs, R. H. *J. Am. Chem. Soc.* **2011**, *133* (22), 8525–8527.

(5) Cannon, J. S.; Grubbs, R. H. *Angew. Chem. Int. Ed.* **2013**, *52* (34), 9001–9004.